

MECHANICAL AND WETTING PROPERTIES OF NANOSILICA/EPOXY-COATED STAINLESS STEEL

MEHANSKE IN POVRŠINSKE LASTNOSTI PREMAZA IZ SILICIJEVIH NANODELCEV IN EPOKSIDNE SMOLE NA NERJAVNEM JEKLU

Marjetka Conradi¹, Gaber Intihar¹, Milena Zorko²

¹Institute of Metals and Technology, Lepi pot 11, 1000 Ljubljana, Slovenia

²National Institute of Chemistry, Hajdrihova 19, 1000 Ljubljana, Slovenia
marjetka.conradi@imt.si

Prejem rokopisa – received: 2015-03-13; sprejem za objavo – accepted for publication: 2015-04-03

doi:10.17222/mit.2015.060

Submicron silica particles surface-capped with diglycidyl ether of bisphenol A were dispersed in a solution of epoxy resin, hardener and acetone. The resulting suspension was then spin-coated onto the surface of austenitic stainless steel of type AISI 316L and cured at temperature, generating a thick silica/epoxy coating 300 nm. An epoxy coating without nanosilica was also prepared as a reference in the same manner. The coatings were further functionalized with fluoroalkylsilane (FAS17) for an additional improvement of the non-wetting properties. The mechanical properties of epoxy coatings filled with different combinations of silica particles 30 nm, 200 nm and 600 nm were compared and characterized using scratch-resistance tests. The effects of incorporating the silica particles on the surface characteristics of the epoxy-coated steel were investigated with contact-angle and surface-energy evaluations. The surface morphology of the coatings was characterized with scanning electron microscopy (SEM). The results indicate that the silica particles significantly improved the microstructure of the coating matrix, which was reflected in an increased damage resistance, a reduced degree of delamination and an induced hydrophobicity. We observed the formation of micrometre-size silica agglomerates as a consequence of the epoxy-matrix curing process. We connected the significantly increased hydrophobicity in silica/epoxy coatings 200 nm and (30 + 600) nm to the proper combination of micro- and nano-roughness created by the agglomerates embedded in the epoxy matrix.

Keywords: silica, composite coatings, scratch test, hydrophobicity

Submikrometrске silicijeve delce, prevlečene z diglicidil etrom bisfenola A, smo dispergirali v raztopini epoksidne smole, utrjevalca in acetona. Nastalo suspenzijo smo nato z vrtenjem nanесли na površino avstenitnega nerjavnega jekla tipa AISI 316L in jo dokončno zamrežili pri povišani temperaturi. Dobili smo 300 nm debelo plast prevleke silicij-epoksidna smola. Tako smo za primerjavo lastnosti pripravili tudi prevleko iz čiste epoksidne smole. Vse prevleke smo dodatno funkcionalizirali s fluoroalkilsilanom (FAS17) za povečanje hidrofobnosti površine. Mehanske lastnosti prevlek iz epoksidne smole, obogatene z različnimi kombinacijami silicijevih delcev 30 nm, 200 nm in 600 nm, smo preizkušali z razenjem. Vpliv vključevanja silicijevih delcev v epoksidno smolo na površinske lastnosti prevlek smo analizirali z meritvami stičnih kotov ter površinske energije. Morfološke lastnosti prevlek smo karakterizirali z vrstično elektronsko mikroskopijo (SEM). Rezultati kažejo, da vključitev silicijevih delcev znatno izboljša mikrostrukturo premaza epoksidne matrike, kar se je pokazalo kot povečana odpornost proti poškodbam, zmanjšanje stopnje delaminacije in inducirane hidrofobnosti. Opazili smo tvorbo silicijevih aglomeratov mikrometrске velikosti kot posledico zamreževanja polimera pri povišani temperaturi. Močno povečano hidrofobnost na površini prevlek silicij-epoksidna smola 200 nm in (30 + 600) nm smo povezali z mikro- in nanohrapavostjo, inducirano s tvorbo aglomeratov v matriki epoksidne smole.

Ključne besede: silika, kompozitne prevleke, preizkus razenja, hidrofobnost

1 INTRODUCTION

In recent decades, polymer composites have started to see uses in many applications as adhesives and matrix resins. Epoxy resin is one of the most common polymer matrices that are widely used to protect steel reinforcements in concrete structures¹. It has excellent mechanical properties, chemical resistance, good electrical insulating properties, and in addition, it also provides an effective physical barrier between the metal and the environment containing an aggressive species, such as an enhanced chloride-ion concentration.

The practical use of epoxy coatings in industry, however, is seriously limited by their poor impact resistance and stress-cracking resistance due to a highly cross-

linked structure², as well as by their susceptibility to damage by surface abrasion and wear³. To overcome this drawback, researchers have made numerous attempts to improve the properties of epoxy by adding various nanofillers⁴⁻⁸. They studied the favourable effects of particle size, volume fraction and the quality of the dispersion on the mechanical response of polymer composites^{4,9-14}.

A lot of work has also been done in the field of modifying the surface wettability through the controlled tailoring of the surface morphology and the surface energy^{15,16}. In this respect, the surfaces were coated with low-surface-energy compounds¹⁷ and/or their roughness was increased, i.e., by etching or nanoparticle deposition^{18,19}. A further technological step is represented by the synthesis of superhydrophobic coatings inspired by

nature (i.e., the lotus leaf). Such coatings are a solution for corrosion, biofouling as well as water- and air-drag reduction applications. Additionally, they improve the mechanical characteristics of the surfaces. For example, nanosilica/epoxy coatings are increasingly attractive and have many potential applications in paints, coatings, sealants, adhesives, etc., due to their low cost, good adhesion to most substrates, good corrosion resistance, good scratch resistance, etc.¹³

Here, we investigate the influence of different sizes of silica nanoparticles (30 nm, 200 nm and 600 nm) on the surface morphology and mechanical characteristics of epoxy coatings on austenitic stainless steel of type AISI 316L. Through the implementation of silica nanoparticles into the epoxy matrix, we focus on a modification of the surface roughness of the epoxy coating that results, in combination with appropriate surface chemistry, in a significantly improved hydrophobicity.

2 EXPERIMENTAL

Materials. – Epoxy resin (Epikote 816, Momentive Specialty Chemicals B.V.) was mixed with a hardener Epikure F205 (Momentive Specialty Chemicals B. V.) in the mass ratio 100 : 53 % and used as the matrix in the composite. Composite-reinforcing silica (SiO₂) nanoparticles with mean diameters of 30 nm were provided by Cab-O-Sil, whereas 200 nm and 600 nm particles were synthesized following the Stöber–Fink–Bohn method in our laboratory²⁰. Diglycidyl ether of bisphenol A (Sigma-Aldrich) was used as the silica-surface modifier to prevent agglomeration. Imidazole (Sigma-Aldrich) served as a reaction catalyst. Austenitic stainless steel of type AISI 316L was used as a substrate.

Surface modification of silica. – Silica and diglycidyl ether of bisphenol A were mixed in the mass ratio 2 : 3 and dispersed in 50 mL of toluene in the presence of imidazole ($w = 25\%$). The mixture was then refluxed at 100 °C for 2 h. To remove the by-product it was centrifuged three times using acetone as a solvent. The remaining silica was then dispersed in acetone and stirred at room temperature for 2–3 h. Finally, the silica was dried in an oven at 110 °C for 2 h.

Steel-substrate preparation. – The steel sheet with a thickness of 1.5 mm was cut into discs with diameters of 25 mm. Prior to the application of the coating, the steel discs were diamond polished following a standard mechanical procedure and then cleaned with ethanol in an ultrasonic bath.

Composite coating preparation. – Epoxy-based composites were prepared by blending with a mass fraction 2 % of 30 nm/200 nm/600 nm surface-modified SiO₂ particles. To improve the dispersion of the silica particles in the coating, they were dispersed in epoxy resin using acetone as a solvent. Prior to the addition of the silica particles, both the resin and the hardener were separately diluted in acetone in a mass ratio of 1 : 4. The nanopar-

ticles were then dispersed in the epoxy resin/acetone solution using ultrasonification for 20–30 min at room temperature. After adding the hardener/acetone solution in the next step, the mixture was manually stirred for a 5 min. Finally, a drop 19 mg of the silica/epoxy resin/hardener/acetone mixture was poured onto the steel substrate disc and a uniform film was then applied to the substrate by a spin-coating process. The composite coatings were then cured in two steps: first pre-cured at 70 °C for 1 h and then post-cured at 150 °C for another hour. The resulting coatings on the steel-substrate plates were thick 300 nm, as determined by ellipsometry. For comparison, neat epoxy coatings without silica fillers were also prepared and cured in the same process as the composites. Finally, to additionally improve the non-wetting properties, the coatings were functionalized by dip-coating in ethanolic fluoroalkylsilane (FAS17, C₁₆H₁₉F₁₇O₃Si, Sigma-Aldrich).

Scanning electron microscopy (SEM). – SEM analysis using FE-SEM Zeiss SUPRA 35VP was employed to investigate the morphology of the silica/epoxy coatings' surfaces.

Scratch test. – The scratch test was performed with a Revetest Scratch tester (CSM Instruments). In the experiment, a scratch length of 10 mm was made using a diamond tip and a linearly increased normal load from 1 N to 5 N at a speed of 5 mm/s. Four tests were performed per sample. A light microscope was employed to analyse the scratches.

Contact-angle and surface-energy measurements. – The static contact-angle measurements of water (W) on a clean AISI 316L diamond-polished sample and on the pure epoxy and silica/epoxy composite coatings prepared on an AISI 316L steel substrate were performed using a surface-energy evaluation system (Advex Instruments s. r. o.). Liquid drops of 5 µL were deposited on different spots of the substrates to avoid the influence of roughness and gravity on the shape of the drop. The drop contour was analysed from the image of the deposited liquid drop on the surface and the contact angle was determined by using Young-Laplace fitting. To minimize the errors due to roughness and heterogeneity, the average values of the contact angles of the drop were calculated approximately 30 s after the deposition from at least five measurements on the studied coated steel. All the contact-angle measurements were carried out at 20 °C and ambient humidity. As the contact angles were only available for water, an equation-of-state approach^{21,22} was used to calculate the corresponding surface energies.

Surface roughness. – A profilometer, model Form Talysurf Series 2 (Taylor-Hobson Ltd.), was employed for the surface analysis. The instrument has a lateral resolution of 1 µm and a vertical resolution of about 5 nm. It measures the surface profile in one direction. TalyMap gold 4.1 software was used for the roughness analysis. The software offers the possibility to calculate

the average surface roughness, S_a , for each sample, based on the general surface-roughness equation:

$$S_a = \frac{1}{L_x} \frac{1}{L_y} \int_0^{L_x} \int_0^{L_y} |z(x, y)| dx dy \quad (1)$$

where L_x and L_y are the acquisition lengths of the surface in the x and y directions and $z(x, y)$ is the height. To level the profile, corrections were made to exclude the general geometrical shape and possible measurement-induced misfits.

3 RESULTS AND DISCUSSION

3.1 Scratch resistance

Typical scratches in the 300 nm thick pure epoxy coating and the 300 nm thick epoxy coating filled with 200 nm silica particles are presented in **Figure 1**. The scratch profile as well as the resistance of the other silica/epoxy coatings is analogous to the 200 nm silica/epoxy coating under investigation, and thus not provided here. It is clear that there is much less displaced material in the case of the silica/epoxy coating compared to the pure epoxy coating. It also seems that the pure epoxy coating is much more brittle than the silica/epoxy coating. This, altogether, indicates that the embedded silica particles can improve the scratch resistance and enhance the toughness of the epoxy coating. In addition, the scratch-test results also suggest that the scratch resistance of the coatings is related to the interaction force between the coating and the steel substrate, which is apparently improved for the silica/epoxy coating.

3.2 Wetting properties

To analyse the surface wettability, five static contact-angle measurements with water (W) were performed on different spots all over the sample and used to determine the average contact-angle values with an estimated error in the reading of $(\theta \pm 1.0)^\circ$ and for the calculation of the surface energy. The wettability, however, was not possible to assess using non-polar liquids for the contact-angle measurements as they spread out on the coatings $(\theta \pm 0^\circ)$. The contact angles and the surface energies for the epoxy and silica/epoxy coatings on the AISI 316L substrate in comparison to the clean, diamond-polished AISI 316L sample are reported in **Table 1**.

It was observed that all the investigated silica/epoxy coatings exhibited significantly higher values of static water-contact angles compared to the clean AISI 316L sample, as well as the AISI 316L substrate blended with pure epoxy. This suggests that the microstructure change of the epoxy coating upon adding the silica particles was reflected in an increased surface roughness, which is known to impart a hydrophobic effect to the surface²³.

The highest values of the static water angles, close to 120° , were however measured in the case of two types of silica/epoxy coatings: 200 nm silica/epoxy coatings and in case of silica/epoxy coatings filled with a combination of 30 nm and 600 nm silica particles. Possible reasons for this observation will be discussed in the following section on surface morphology and surface roughness.

Table 1: Surface properties of diamond-polished AISI 316L substrate and AISI 316L substrate when blended with pure epoxy and various types of silica/epoxy coatings. Static contact angles were measured with water (θ^W) and the corresponding surface energies were calculated using an equation-of-state approach.

Tabela 1: Površinske lastnosti z diamantno pasto polirane površine podlage AISI 316L in AISI 316L, prevlečne s čisto epoksidno smolo in različnimi prevlekami iz silicij-epoksidne smole. Statični stični koti so bili izmerjeni z vodo (θ^W), ustrezne površinske energije pa so bile izračunane z enačbo stanja.

Substrate	Contact angle $\theta^W/^\circ$	Surface energy $\gamma^{tot}/(mN/m)$
AISI	68.4	42.7
AISI + epoxy	80.2	35.4
AISI + 30 nm silica/epoxy	110.1	17.0
AISI + 200 nm silica/epoxy	117.7	12.8
AISI + 600 nm silica/epoxy	110.1	17.0
AISI + (30 + 200) nm silica/epoxy	111.7	16.1
AISI + (200 + 600) nm silica/epoxy	111.0	16.5
AISI + (30 + 600) nm silica/epoxy	118.4	12.5

As the contact angles were only available for water, an equation-of-state approach^{21,22} was used to calculate the surface energies with Equation (1):

$$\cos \theta = -1 + 2 \sqrt{\frac{\gamma_s}{\gamma_1}} e^{-\beta(\gamma_1 - \gamma_s)^2} \quad (2)$$

For a given value of the surface tension of the probe liquid γ_1 (i.e., for water $\gamma_1 = 72.8 \text{ mN/m}$ ²⁴) and θ^W measured on the same solid surface, the constant β and

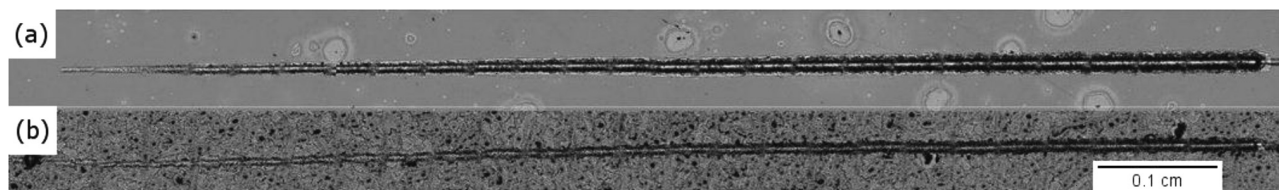


Figure 1: Light micrographs revealing the typical morphology of scratches: a) for the thick pure epoxy coating 300 nm on AISI 316L and b) for the thick epoxy coating 300 nm filled with silica particles 200 nm on AISI 316L

Slika 1: Svetlobna mikroskopija prikazuje značilno morfologijo prask: a) na 300 nm debeli prevleki iz čiste epoksidne smole in b) na 300 nm debeli prevleki iz epoksidne smole, obogatene s silicijevimi delci 200 nm

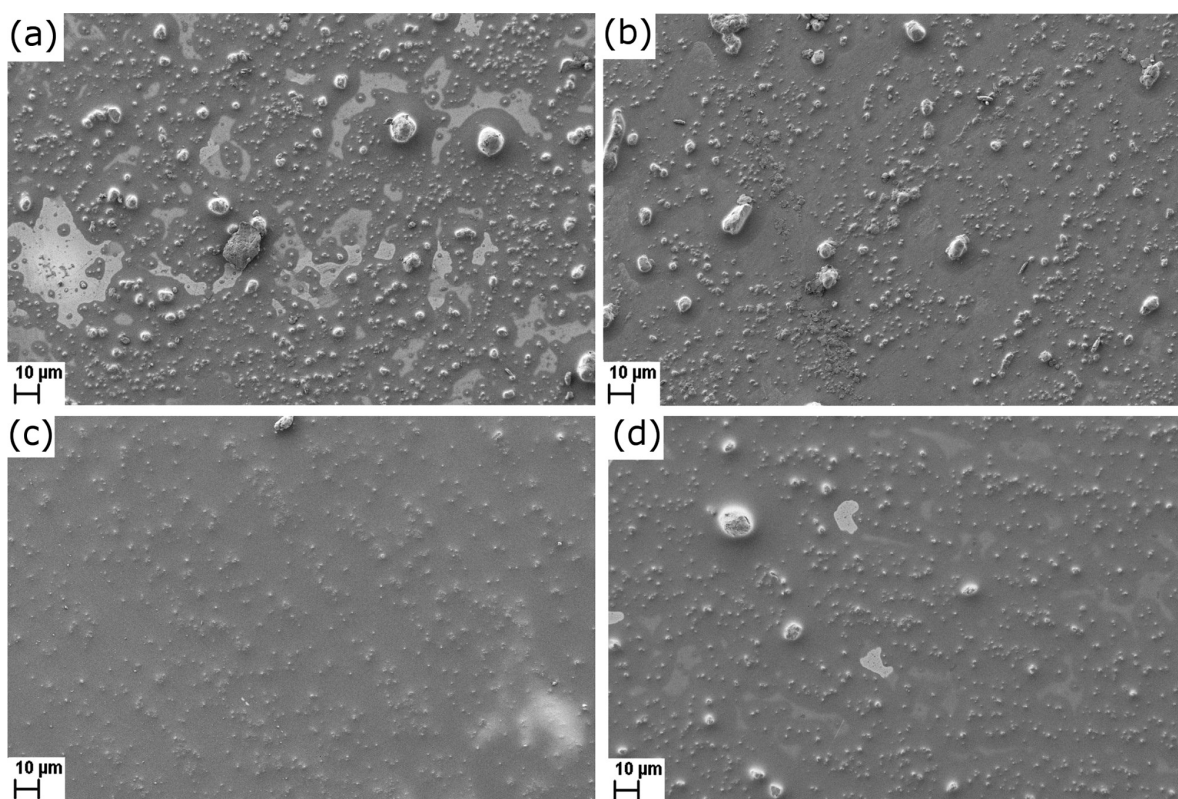


Figure 2: SEM images of AISI 316L substrate when blended with: a) silica/epoxy 30 nm, b) silica/epoxy 200 nm, c) silica/epoxy 600 nm and d) silica/epoxy coating (30 + 600) nm

Slika 2: SEM-posnetki podlage AISI 316L, prevlečene s prevlekami iz: a) 30 nm silicij-epoksidne smole, b) 200 nm silicij-epoksidne smole, c) 600 nm silicij-epoksidne smole in d) (30 + 600) nm silicij-epoksidne smole

the solid surface-tension γ_s values were determined using the least-squares analysis technique. For the fitting with Equation (2), a literature value of $\beta = 0.0001234$ (mJ/m²)⁻² was used, as weighted for a variety of solid surfaces²². Again, the calculated values of the solid surface energy (**Table 1**) dropped significantly when the clean AISI 316L substrate was covered with silica/epoxy coatings, confirming the induced surface hydrophobicity. The low surface energy of the silica/epoxy coatings is most probably a consequence of the combination of silica-induced surface roughness and the appropriate surface chemistry due to the coatings' functionalization with fluoroalkylsilane.

3.3 Surface morphology

Figure 2 compares the typical morphology of various silica-epoxy coatings. It is clear that in spite of the silica-surface modification with an epoxy-compatible component, we could not prevent silica agglomeration in the coating. After several different attempts we came to the conclusion that the agglomeration appears during the curing process and is most probably a consequence of solvent (acetone) evaporation, together with the formation of a highly cross-linked epoxy structure.

A detailed look at the surface morphology, however, brought us to the conclusion that there exists a typical

average agglomerate size, which depends on the size of the silica fillers in the epoxy matrix. These agglomerates, which are typically in the μm size range, consequently

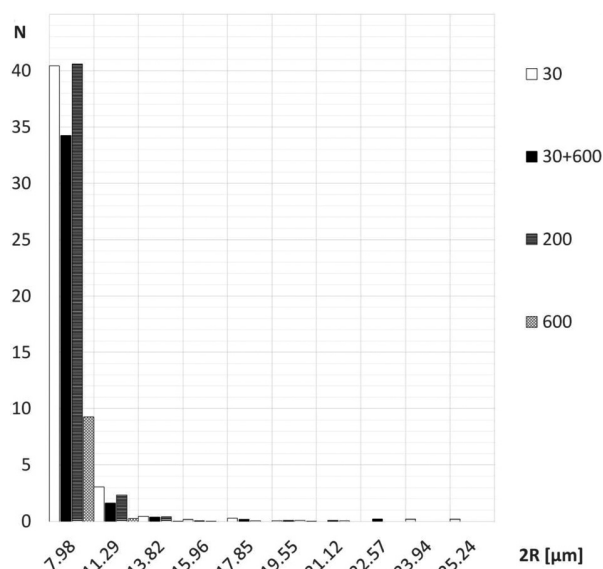


Figure 3: Size distribution of silica agglomerates in 30 nm, 200 nm, 600 nm and (30 + 600) nm silica/epoxy coatings

Slika 3: Velikostna porazdelitev silicijevih aglomeratov v prevlekah iz epoksidne smole, obogatene s silicijevimi nanodelci 30 nm, 200 nm, 600 nm in (30 + 600) nm

create a micro-roughness on top of the nano-roughness created by the individual silica nanoparticles embedded in the epoxy matrix. As is already known, it is the combination of the two, i.e., the micro- and the nano-roughness, that increases the static water contact angle and makes the surface more hydrophobic²⁵.

As reported in **Table 1**, we measured the highest static water contact angles, close to 120 °, only on the surfaces of the 200 nm and (30 + 600) nm silica/epoxy coatings. In **Figure 3** we can see that these two coatings are characterized mostly with agglomerates having diameters of 8 µm and 11 µm. The same holds for the morphology of the 30 nm silica/epoxy coating; however, here we also observe an inconsiderable number of larger agglomerates that most probably influence the proper ratio between the micro- and nano-roughness necessary for an increase of the static water contact angle. This suggests the agglomerate/nanoparticle ratio is extremely sensitive to the appropriate surface roughness that will create a hydrophobic/superhydrophobic surface. This result also confirms the competitive importance of the surface morphology on the wetting properties compared to a low surface energy tailored with the surface chemistry.

3.4 Surface Roughness

Finally, we confirmed the morphology observations and determined the effect of the incorporation of silica on the morphology of the epoxy coating, by measuring the average surface roughness of the coatings, S_a . An examination of the silica/epoxy-coated steel surface with a profilometer revealed that the nanoparticles' size significantly influences the coating's roughness and consequently the morphology of the surface. As listed in **Table 2**, S_a of 200 nm and (30 + 600) nm silica/epoxy coatings is of the same order of magnitude and in the intermediate regime compared to 30 nm and 600 nm silica/epoxy coatings. This is consistent with the observation of the average size of the agglomerates characterizing the morphology of each coating, as reported in the previous section. Here, we have shown that an intermediate roughness gives the best results in terms of an increased hydrophobicity (**Tables 1** and **2**). Moreover, this confirms the importance of the appropriate surface roughness on the wetting behaviour of the coatings.

Table 2: Average surface roughness, S_a , of various silica/epoxy coatings on an AISI 316L substrate

Tabela 2: Povprečna površinska hrapavost S_a različnih prevlek iz silicij-epoksidne smole na podlagi AISI 316L

Substrate	S_a
AISI + 30 nm silica/epoxy	0.65
AISI + 200 nm silica/epoxy	0.41
AISI + 600 nm silica/epoxy	0.27
AISI + (30 + 600) nm silica/epoxy	0.46

4 CONCLUSIONS

Nanosilica particles were homogeneously dispersed in an epoxy matrix at a mass concentration of 2 % and mixtures with different combinations of 30 nm, 200 nm and 600 nm silica were successfully spin coated on austenitic stainless steel of type AISI 316L to form a 300 nm coating. For an additional improvement of the non-wetting properties, the coatings were functionalized by dip-coating in ethanolic fluoroalkylsilane (FAS17).

The mechanical properties of the coatings were evaluated with a scratch test, indicating that the more brittle pure epoxy coating underwent more severe damage, accompanied by a pronounced material displacement compared to the silica/epoxy coating. This indicates that the silica particles enhanced the toughness of the epoxy coating.

The silica nanoparticles changed the microstructure of the epoxy coating, which was reflected in an increased roughness of the silica/epoxy-coated AISI 316L sample. The increased hydrophobicity of the silica/epoxy coatings, on the other hand, was a consequence of the combination of silica-induced surface roughness and the appropriate surface chemistry, due to the coatings' functionalization with fluoroalkylsilane.

The surface morphology of the silica/epoxy coatings was characterized by the formation of micrometre-size silica agglomerates as a consequence of the epoxy-matrix curing process. The significantly increased hydrophobicity in the 200 nm and (30 + 600) nm silica/epoxy coatings was connected to the proper combination of micro- and nano-roughness created by the agglomerates embedded in the epoxy matrix.

Acknowledgement

This work was carried out within the framework of the Slovenian programme P2-0132, "Fizika in kemija površin kovinskih materialov" of the Slovenian Research Agency, whose support is gratefully acknowledged by M. Conradi.

5 REFERENCES

- F. Galliano, D. Landolt, Evaluation of corrosion protection properties of additives for waterborne epoxy coatings on steel, *Prog. Org. Coat.*, 44 (2002), 217–225, doi:10.1016/S0300-9440(02)00016-4
- S. Yamini, R. J. Young, Stability of crack-propagation in epoxy-resins, *Polymer*, 18 (1977) 10, 1075–1080, doi:10.1016/0032-3861(77)90016-7
- B. Wetzel, F. Hauptert, M. Q. Zhang, Epoxy nanocomposites with high mechanical and tribological performance, *Comp. Sci. Tech.*, 63 (2003), 2055–2067, doi:10.1016/S0266-3538(03)00115-5
- A. C. Moloney, H. H. Kausch, T. Kaiser, H. R. Beer, Parameters determining the strength and toughness of particulate filled epoxide-resins, *J. Mat. Sci.*, 22 (1987), 381–393, doi:10.1007/BF01160743
- E. P. Giannelis, Polymer-layered silicate nanocomposites: Synthesis, properties and applications, *App. Org. Chem.*, 12 (1998), 675–680, doi:10.1002/(SICI)1099-0739(199810/11)12:10<675::AID-AOC779>3.0.CO;2-V

- ⁶ T. Lan, T. J. Pinnavaia, Clay-reinforced epoxy nanocomposites, *Chem. Mat.*, 6 (1994), 2216-2219, doi:10.1021/cm00048a006
- ⁷ R. P. Singh, M. Zhang, D. Chan, Toughening of a brittle thermosetting polymer: Effects of reinforcement particle size and volume fraction, *J. Mat. Sci.*, 37 (2002), 781-788, doi:10.1023/A:1013844015493
- ⁸ R. A. Pearson, A. F. Yee, Influence of particle-size and particle-size distribution on toughening mechanisms in rubber-modified epoxies, *J. Mat. Sci.*, 26 (1991), 3828-3844, doi:10.1007/BF01184979
- ⁹ M. Frounchi, T. A. Westgate, R. P. Chaplin, R. P. Burford, Fracture of polymer networks based on diethylene glycol bis(allyl carbonate), *Polymer*, 35 (1994), 5041-5045, doi:10.1016/0032-3861(94)90661-0
- ¹⁰ R. T. Quazi, S. N. Bhattacharya, E. Kosior, The effect of dispersed paint particles on the mechanical properties of rubber toughened polypropylene composites, *J. Mat. Sci.*, 34 (1999), 607-614, doi:10.1023/A:1004515300637
- ¹¹ T. Adachi, W. Araki, T. Nakahara, A. Yamaji, M. Gamou, Fracture toughness of silica particulate-filled epoxy composite, *J. App. Polym. Sci.*, 86 (2002), 2261-2265, doi:10.1002/app.11206
- ¹² A. Boonyapookana, K. Nagata, Y. Mutoh, Fatigue crack growth behavior of silica particulate reinforced epoxy resin composite, *Comp. Sci. Tech.*, 71 (2011), 1124-1131, doi:10.1016/j.compscitech.2011.02.015
- ¹³ J. Yuan, S. Zhou, G. Gu, L. Wu, Effect of particle size of nanosilica on the performance of epoxy/silica composite coatings, *J. Mat. Sci.*, 40 (2005), 3927-3932, doi:10.1007/s10853-005-0714-8
- ¹⁴ M. Conradi, M. Zorko, A. Kocijan, I. Verpoest, Mechanical properties of epoxy composites reinforced with a low volume fraction of nanosilica fillers, *Mat. Chem. Phys.*, 137 (2013), 910-915, doi:10.1016/j.matchemphys.2012.11.001
- ¹⁵ A. Tuteja, W. Choi, M. Ma, J. M. Marby, S. A. Mazzella, G. C. Rutledge, G. G. McKinley, R. E. Cohen, Designing superoleophobic surfaces, *Science*, 318 (2007), 1618-1622, doi:10.1126/science.1148326
- ¹⁶ C. H. Xue, S. T. Jia, J. Zhang, L. Q. Tian, H. Z. Chen, M. Wang, Preparation of superhydrophobic surfaces on cotton textiles, *Sci. Technol. Adv. Mater.*, 9 (2008) 3, 035008, doi:10.1088/1468-6996/9/3/035008
- ¹⁷ A. Zenerino, T. Darmanin, E. T. deGivenchy, S. Amigoni, F. Guittard, Connector ability to design superhydrophobic and oleophobic surfaces from conducting polymers, *Langmuir*, 26 (2010), 13545-13549, doi:10.1021/la101734s
- ¹⁸ N. Salema, D. K. Sarkar, R. W. Paynter, X. G. Cheng, Superhydrophobic aluminum alloy surfaces by a novel one-step process, *ACS Appl. Mater. Interfaces*, 2 (2010), 2500-2502, doi:10.1021/la104979x
- ¹⁹ Z. Guo, X. Chen, J. Li, J. H. Liu, X. J. Huang, ZnO/CuO hetero-hierarchical nanotrees array, hydrothermal preparation and self-cleaning properties, *Langmuir*, 27 (2011), 6193-6200, doi:10.1021/la104979x
- ²⁰ W. Stober, A. Fink, E. Bohn, Controlled growth of monodisperse silica spheres in micron size range, *Journal of Colloid and Interface Science*, 26 (1968), 62-69, doi:10.1016/0021-9797(68)90272-5
- ²¹ D. Li, A. W. Neumann, A reformulation of the equation of state for interfacial-tensions, *Journal of Colloid and Interface Science*, 137 (1990), 304-307, doi:10.1016/0021-9797(90)90067-X
- ²² D. Y. Kwok, A. W. Neumann, Contact angle measurement and contact angle interpretation, *Advances in Colloid and Interface Science*, 81 (1999), 167-249, doi:10.1016/S0001-8686(98)00087-6
- ²³ J. Y. Shiu, C. W. Kuo, P. L. Chen, C. Y. Mou, Fabrication of tunable superhydrophobic surfaces by nanosphere lithography, *Chem. Mat.*, 16 (2004), 561-564, doi:10.1021/cm034696h
- ²⁴ Y. Y. Yu, C. Y. Chen, W. C. Chen, Synthesis and characterization of organic - inorganic hybrid thin films from poly(acrylic) and monodispersed colloidal silica, *Polymer*, 44 (2003), 593-601, doi:10.1016/S0032-3861(02)00824-8
- ²⁵ T. J. Athauda, W. Williams, K. P. Roberts, R. R. Ozer, On the surface roughness and hydrophobicity of dual-size double-layer silica nanoparticles, *J. Mater. Sci.*, 48 (2013) 18, 6115-6120, doi:10.1007/s10853-013-7407-5